Numerical simulations of atmospheric dispersion of large-scale liquid hydrogen releases

Baopeng Xu[1], Simon Jallais[2], Deborah Houssin[2], Elena Vyazmina[2], Laurence Bernard[2] and Jennifer X. Wen[1,*]

[1]Warwick FIRE, School of Engineering, University of Warwick, Coventry, CV4 7AL, UK

[2]Air Liquide Innovation Campus Paris 78354 Jouy en Josas, France

[*]Email address for correspondence: Jennifer.wen@warwick.ac.uk

Abstract

Numerical simulations have been conducted for LH_2 massive releases and the subsequent atmospheric dispersion using an in-house modified version of the open source computational fluid dynamics (CFD) code OpenFOAM. A conjugate heat transfer model has been added for heat transfer between the released LH_2 and the ground. Appropriate interface boundary conditions are applied to ensure the continuities of temperature and heat fluxes. The significant temperature difference between the cryogenic hydrogen and the ground means that the released LH_2 will instantly enter in a boiling state, resulting in a hydrogen- air gaseous cloud, which will initially behave like a dense gas. Numerical predictions have been conducted for the subsequent atmospheric dispersion of the vaporized LH_2 for a series of release scenarios - with and without retention pits - to limit the horizontal spread of the LH_2 on the ground. The considered cases included the instantaneous release of 1, 10 and 50 tons of LH_2 under neutral (D) and stable (F) weather conditions. More specifically, 3F and 5D conditions were simulated with the former representing stable weather conditions under wind speed of 3 m/s at 10 m above the ground and the later corresponding to neutral weather conditions under 5 m/s wind speed (10 m above the ground). Specific numerical tests have also been conducted for selected scenarios under different ambient temperatures from 233 up to 313 K. According to the current study, although the retention pit can extend the dispersion time, it can significantly reduce the extent of hazards due to much smaller cloud size within both the flammability and explosion limits. While the former has negative impact on safety, the later is beneficial. The use of retention pit should hence be considered with caution in practical applications.

1. Introduction

As a clean energy carrier, hydrogen has the potential to participate in alleviating the current rapid climate change. To increase its volumetric energy density, hydrogen tends to be stored in cryogenic liquid form at a temperature as low as 20.4 K. The instantaneous rupture of a LH_2 tank poses a great hazard due to the low temperature.

The abrupt depressurization of a large amount of LH_2 would potentially lead to the formation of a LH_2 pool, accompanying a spontaneous flash evaporation. The LH_2 in the pool is heated

via the heat transfer from the solid ground/walls, ambient air and the sun radiation. In the initial stage of the evaporation process, the conduction heat transfer via the ground is the major contribution due to the very large temperature difference, which results in fast vaporization due to the violent boiling. The evaporated gaseous hydrogen is dispersed in the ambient air, forming a dense cloud. The hydrogen temperature is lower than the liquefaction/solidification temperature of the air components, causing foreseeable phase changes. More importantly, the dispersion of the evapourated hydrogen would result in the formation of a flammable/explosive cloud, posing a safety issue which needs to be addressed to minize the potential risk to the public. In such context, the accurate prediction of the atmospheric hydrogen distribution is an important step to assess accurately the hazards of storage systems.

Numerical prediction of the atmospheric dispersion requires the determination of the pool size and evaporation rate being inlet conditions. The inlet conditions are closely related to the release models. The catastrophic failure of a storage tank is the most dangerous release scenario, which causes an instantaneous release of LH_2. It is hence prudent to consider such events as worst case scenarios during design stage. To delay the spread of LH_2 and limit the vaporization rate, a detention pit is considered to minimize the size of the flammable vapor cloud. The present study numerically investigate the atmospheric dispersion of vaporized LH_2 for the instantaneous release scenarios in the situations of with/without the detention pits. Following validation using data from NASA LH_2 tests [1], the numerical predictions were used to analyse the effects of ambient temperature, atmospheric conditions and the presence of a retention pit on flammable cloud dispersion and associated potential hazardous distances.

2. Numerical formulations

2.1 Flow solver

Numerical modeling of LH_2 releases and the subsequent atmospheric dispersion is challenging, particularly for the phase change dynamics. The mixing of cryogenic hydrogen with ambient air can result in the phase transition of oxygen and nitrogen at the near-field, which is too complicated to be directly modeled due to the cryogenic condition and lack of detailed experimental data for model validation. However, as the phase transition of oxygen and nitrogen occurs only at the near-field, its influence on the far-field dispersion can be assumed to be relatively small. Furthermore, the condensation of water vapor prevails in the dispersion process of the evoporated cold hydrogen gas, which releases its latent heat to increase the cloud buoyancy. It was also experimentally revealed that the warming from the mixing with air plays a major role in the buoyancy effect. This effect is also neglected in the current study, which is focused on investiagitng the effects of detention pits in comparison with the same release scenarios withou the rention pits. The influence of humidity on the buoyancy of coud dispersion and most importantly the horizontal and vertical extent of the flammable coud will be investigated in our future study.

Three-dimensional multi-component compressible Navier-Stokes equations in the Reynold Averaged context (RANS) are formulated to model the atmospheric dispersion:

$$\frac{\partial \rho}{\partial t} + \nabla \cdot \left(\underline{\rho}\underline{u}\right) = 0$$

$$\frac{\partial \underline{\rho}\underline{u}}{\partial t} + \nabla \cdot \left(\underline{\rho}\underline{u}\underline{u}\right) = -\Delta \underline{p} + \nabla \cdot \underline{\tau_{eff}} + \underline{\rho} g$$

$$\frac{\partial \underline{\rho} Y_i}{\partial t} + \nabla \cdot \left(\underline{\rho}\underline{u}\underline{Y_i}\right) = \nabla \cdot \left(\mu_{eff} \underline{Y_i}\right)$$

$$\frac{\partial \underline{\rho} h_s}{\partial t} + \nabla \cdot \left(\underline{\rho}\underline{u}\underline{h_s}\right) = \nabla \cdot \left(\alpha_{eff} \nabla \underline{h_s}\right) + \sum_{i=1}^{n} \quad \left(\nabla \cdot \underline{h_{si}} [\rho D_i - \alpha] \nabla \underline{Y_i}\right)$$

$$\frac{\partial \left(\underline{\rho} k\right)}{\partial t} + \nabla \cdot \left(\underline{\rho}\underline{u} k\right) = \nabla \cdot \left[\left(\frac{\mu_{eff}}{Pr_k}\right) \nabla k\right] + P_k + G_k - \underline{\rho}\varepsilon$$

$$\frac{\partial \left(\underline{\rho}\varepsilon\right)}{\partial t} + \nabla \cdot \left(\underline{\rho}\underline{u}\varepsilon\right) = \nabla \cdot \left[\left(\frac{\mu_{eff}}{Pr_\varepsilon}\right) \nabla \varepsilon\right] + \frac{\varepsilon}{k} (C_{\varepsilon 1} P_k + C_{\varepsilon 1} C_{\varepsilon 3} G_k - C_{\varepsilon 2} \varepsilon)$$

In the above formulations the turbulent effect is modeled by standard time-averaged $k - \varepsilon$ model.

2.2 Conjugate heat transfer model

The evapourated cold hydrogen gas initially behave like dense gas following the release. Heat transfer from the ground to the dispersed cloud increases its temperature and promotes buoyancy effect. To capture this process, a conjugate heat transfer model, which solves the fluid region and the ground region separately, is coupled with the interface boundary conditions which ensure the continuities of temperature and heat flux at the interfaces.

The governing equation for the heat transfer in the ground is written as:

$$\rho C_p \frac{\partial T_g}{\partial t} = \nabla \cdot (k \nabla T_g)$$

At the interface between the fluid and ground the following equations apply:

$$T_{f,int} = T_{g,int}$$

$$\dot{Q}_{con} = k_g \frac{\partial T_g}{\partial y} \Big|_{int, y=-0}$$

The convective heat transfer coefficient is calculated according to an empirical equation [2] which is valid for wind speed from 2-20 m/s:

$$h_c = 10.45 - u + 10\sqrt{u}$$

2.3 Vaporization rate

In this study, the worst case scenario, i.e. the instantaneous release of all the content in the storage tank, is considered. For spills on ground, the initial stage of vaporization is controlled by the heat conduction from the ground. As the initial temperature difference between the cryogenic hydrogen and the ground is very large, the LH_2 will be instantly in a boiling state. Accurate prediction of the boiling heat transfer under cryogenic conditions need to address the complex underlying physics, which requires the incorporation of all heat and mass transfer components. In this comparative study for cases with and without the detention pit, a simplified equation to calculate the heat flux from the ground into the LH_2 is used by making the following assumptions:

(a) The initial temperature has a uniform temperature T_0;

(b) The outer ground temperature experiences a sudden drop to the temperature T_1;

(c) The temperature will not change at an infinite distance from the inside surface.

The time-dependent heat flux can be calculated by a simple analytical solution and given as:

$$H_c(t) = \frac{\lambda(T_0 - T_b)}{\sqrt{a \cdot \pi \cdot t}}$$

where T_0 is initial temperature of ground, T_b is boiling point of hydrogen, λ is thermal conductivity of ground, $a = \lambda/(\rho.C_p)$, ρ and C_p are density and specific heat of ground respectively. The heat conduction flux from the subsoil at the initial stage is much larger than the heat flux due to other sources. So, by neglecting the small terms in the heat balance, the vaporization rate of LH_2 is then determined by $\dot{q}_v = H_c(t)/L_v$. The vaporization rate is inversely proportional to the square root of time.

It should be noted that the effect of the spreading process, which inevitably causes delay in the contact between the cold LH_2 and warm subsoil, is neglected as a compromise between computational time, complexity and resouces. To avoid an unrealistic high predicted evaporation rate in the initial stages of the spill $t \approx 0$, an articial delay time was used. For the cases without pit, the delay time was assumed 20 seconds and 10 seconds were used for cases with pits.

As long as the liquid pool is boiling, its (average) temperature remains constant at normal boiling point, and no latent heat of the pool is withdrawn. The heat conduction flux from the subsoil at the initial stage is much larger than the heat flux due to other sources. So, by neglecting the small terms in the heat balance, the vaporization rate of LH_2 can be calculated by $\dot{q}_v = H_c(t)/L_v$. The vaporization rate is inversely proportional to the square root of time.

2.4 The atmospheric boundary model

The atmospheric dispersion is closely related to the atmospheric boundary layer conditions, which are specified throguh the wind inlet profiles for velocity and turbulent conditions. These profiles are parameterized as the atmospheric stability according to the Pasquill-Gifford stability classes [4], which rates from class A (unstable) through D (neutral) to F (stable).

According to Van den Bosch [3] , the velocity profile is written as:

$$U(z) = \frac{u^*}{k}\left[ln\left(\frac{z}{z_0}\right) - \varphi_m\right]$$

Where u^* is the friction velocity, given by:

$$u^* = \frac{U_0 k}{ln\left(\frac{z_{ref}}{z_0}\right) - \varphi_m}$$

Where U_0 is the wind velocity at the reference height z_{ref}. The stability function φ_m is calculated by:

$$\varphi_m = \{2ln\left(\frac{1+\gamma}{2}\right) + ln\left(\frac{1+\gamma^2}{2}\right) - 2arctan(\gamma) + \frac{\pi}{2} \quad if\ L < 0 \\ -17\left[1 - exp\left(-0.29\frac{z}{L}\right)\right] \qquad if\ L \geq 0$$

Where $\gamma = \left(1 - 16\frac{z}{L}\right)^{\frac{1}{4}}$.

The profiles of the turbulent kinetic energy k and turbulence dissipation rate ε for the neutral and stable atmospheric boundary conditions are defined by:

$$k(z) = \{6u^{*2} \qquad if\ z \leq 0.1h_{abl} \\ 6u^{*2}\left(1 - \frac{z}{h_{abl}}\right)^{1.75} \quad if z > 0.1h_{abl}$$

$$\varepsilon(z) = \{\frac{u^{*3}}{kz}\left(1.24 + 4.3\frac{z}{L}\right) \qquad if\ z \leq 0.1h_{abl} \\ \frac{u^{*3}}{kz}\left(1.24 + 4.3\frac{z}{L}\right)(1 - 0.85z \cdot h_{abl}) \quad if z > 0.1h_{abl}$$

$$h_{abl,neutral} = 0.3\frac{u^*}{f_c}$$

$$h_{abl,stable} = 0.4\left(\frac{u^* L}{f_c}\right)^{\frac{1}{2}}$$

In this study, only neutral and stable boundary layer conditions are considered.

3. Problem descriptions

Following the instantaneous release, flash evaporation occurs prior to the formation of the liquid pool. In this study, this process is neglected by assuming that the temperature of the stored LH_2 is equal to the boiling point at the atmospheric condition. The pool spreading is

closely related to initial release momentum resulting from the abrupt rupture. For the instantaneous release, it is difficult to quantify the initial momentum. It is hence assumed that the LH_2 spreads instantaneously to the minimum thickness and reaches its maximum pool size immediately. This simplified assumption can lead to over-predictions of the vaporization rate shortly after the release. The minimum thickness is related to the surface roughness varying from 5 mm to several centimeters. In this study a minimum thickness of 5 cm is chosen. The presence of a retention pit reduces the vaporization rate by limiting the pool area. In the presence of the retention pit, the LH_2 content is assumed to fill the pit instantaneously. The release scenarios of both with and without retention pits are numerically simulated for comparison.

Table 1 Summary of the cases considered

Release scenarios	Content (T)	Pool size (m×m)	Weather condition	Ambient temperature (K)
With retention pit	1	4.5×6	3F, 5D	253, 273, 293
	1	3.5×5	3F, 5D	293
	10	6×14	3F, 5D	253, 273, 293
	10	5×13	3F, 5D	293
Without retention pit	1	17×17	3F, 5D	253, 273, 293
	3	29×29	3F, 5D	293
	5	37.5×37.5	3F, 5D	293
	10	53×53	3F, 5D	253, 273, 293
	50	118×118	3F, 5D	293

The LH_2 dispersion is affected by several factors, such as wind speed, atmospheric stability, ambient temperature, and the amount of the released content, etc. The effect of these parameters is systematically investigated for different release quantities, representing different sizes of the storage tanks. A summary of the considered cases are listed in Table 1. A square pool is assumed to facilitate meshing and to speed up the simulations. A total of 34 cases were simulated as listed in Table 1. The atmospheric stability according to the Pasquill-Gifford stability classes rates from class A (unstable) through D (neutral) to F (stable). In the present study, 3D and 5F have been considered for each release scenario. Here, 3 and 5 represent the wind velocity of 3m/s and 5m/s, respectively. It should be noted that the pit height was not considered. In the computational setup, the pit is used as an inlet boundary where a time-dependent mass flow rate and a constant boiling temperature were applied. Such treatment implicitly assumes that the pit is sufficiently high to contain the intial LH2. To assist the detailed design of the pit, more detailed numerical simulations should be conducted to incoporate the physical processes in the transient release processes.

The computational domain is shown in Figure 1. The grid is non-uniform with higher resolutions concentrated near the groud and immediately above the LH_2 pool. The effect of the pit geometry is neglected and an inlet boundary for the vaporized hydrogen is placed 10 m downstream the wind inlet boundary at the ground level. The instantaneous releases and LH_2 pools are assumed to form instantaneously. The vaporization rate is different for the two release scenarios: a transient vaporization rate is applied to the cases with retention pit, and a steady rate is used for the cases without retention pit due to its short vaporization time.

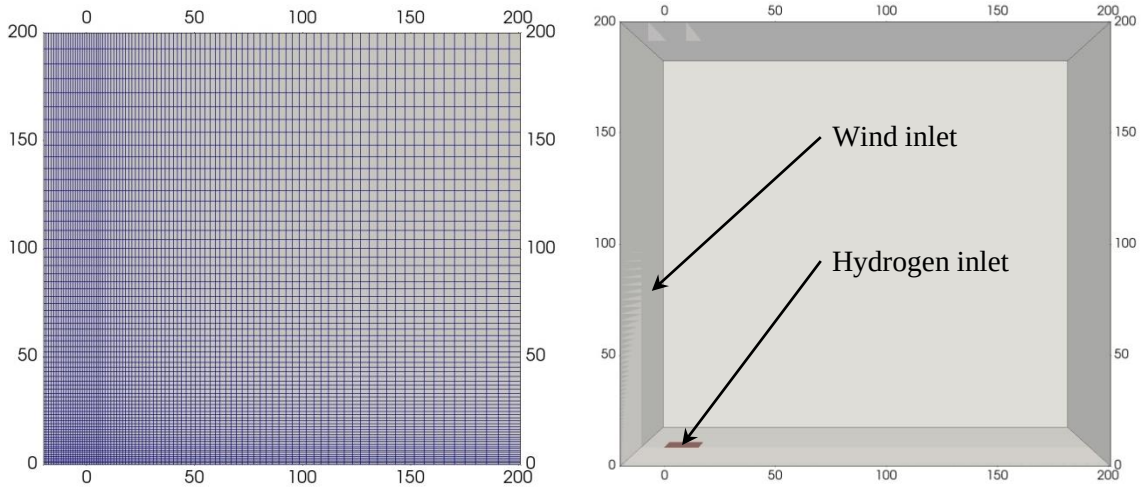

Fig.1 The computational grid.

Results and discussion

Figure 2 shows the comparison between the current predictions and the NASA experimental measurements of Witcofski and Chirivella [1] at =20.9 s. It was found that drastic changes in H_2 concentration could occur within only 0.4 s in the test [1]. The predicted cloud shape is similar to that of the experimental observation, although the predicted cloud travels further than the test cloud due to the assumption of instantaneous release. In the NASA test, the visible cloud of 6.7% H_2 was recorded to extend as far as 160 m and as high as 65 m; and remained visible for 90 s. In the predicted contours of the hydrogen concentration, the predicted extent of the 6.7% H_2 reached 162 m, 66 m at 90 s, in good agreement with the experimental observations.

Fig. 2 Comparison between the current predictions and the NASA experimental measurements of Witcofski and Chirivella [1]

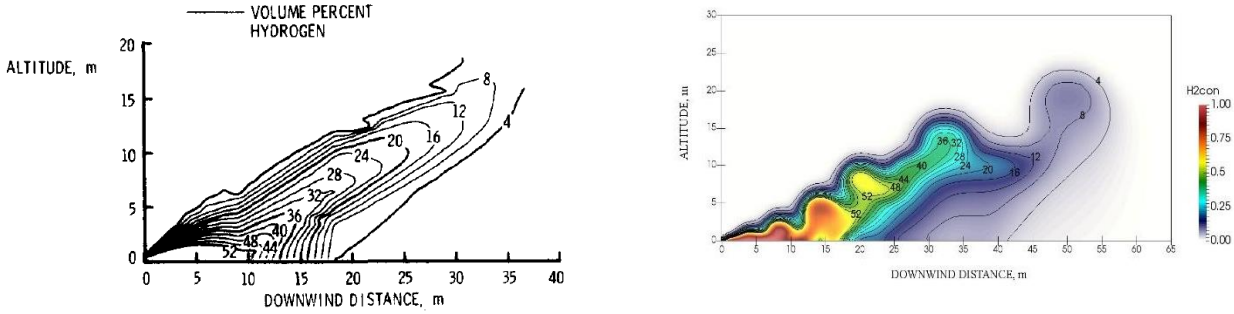

at t=20.9 s.

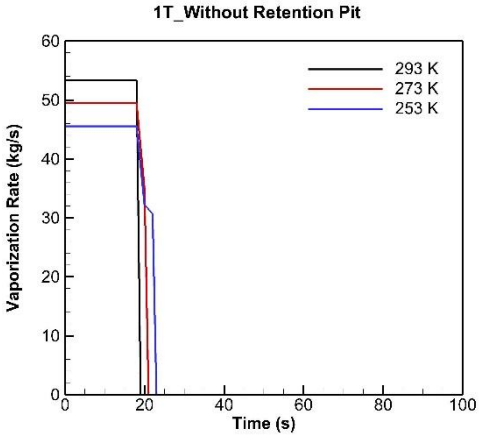

Fig. 3 The predicted vaporization rate for 1 ton LH_2 release at different ambient temperatures.

Figure 3 shows the predicted vaporization rate for 1 ton LH_2 release at different ambient temperatures. It is seen that the ambient temperature affects the vaporization rate, especially the peak values which are reached quickly after the release. As the cloud is only dense close to the release point and quickly becomes neutral due to mixing with air. It is expected that the evaporation rate plays a more important role than buoyancy for the subsequent cloud evolution. It can also be seen that the retention pit can significantly reduce the vaporization rate and extend the vaporization time. While the former is positive for safety concern, the later can potentially offset any potential benefit as the extended vaporization time would increase the propabaility of ignition.

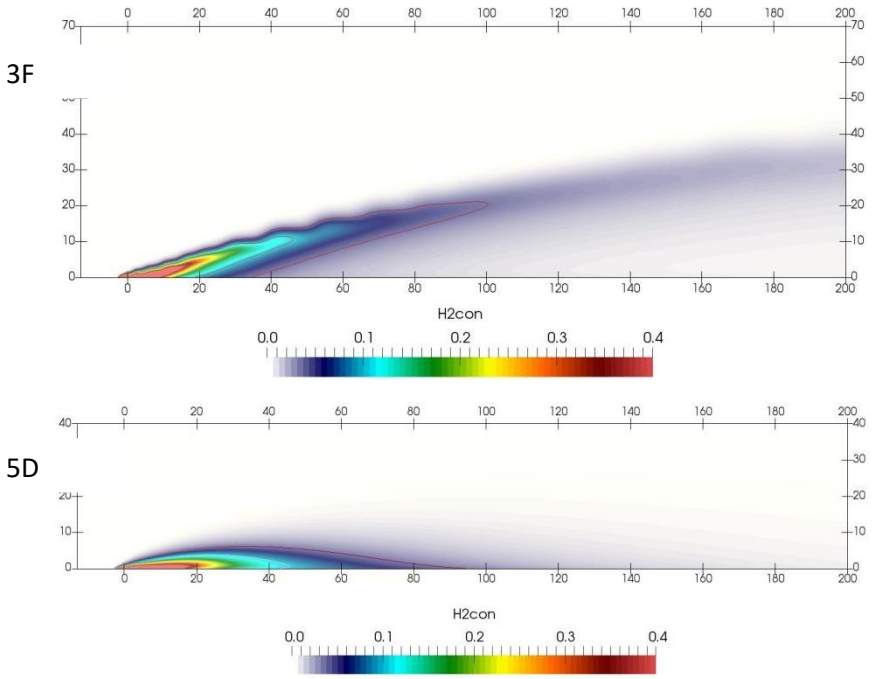

Fig. 4 The predicted dispersion of the 1 ton cloud at ambient temperature 293 K at t =100 s. The red line denotes 4% molar concentration.

Figure 4 shows that the predicted cloud lifts off the ground for the weather condition of 3F, and the predicted cloud of 5D is found to travel along the ground level. Although the prediced

cloud of 5D falls on the ground, the cloud within the flamibility limit travels almost the same distance as that of the case 3F. It is also revealed by the simulations that the predicted cloud is observed to gradually reduce after the formation of the largest cloud due to the decreasing vaporation rate.

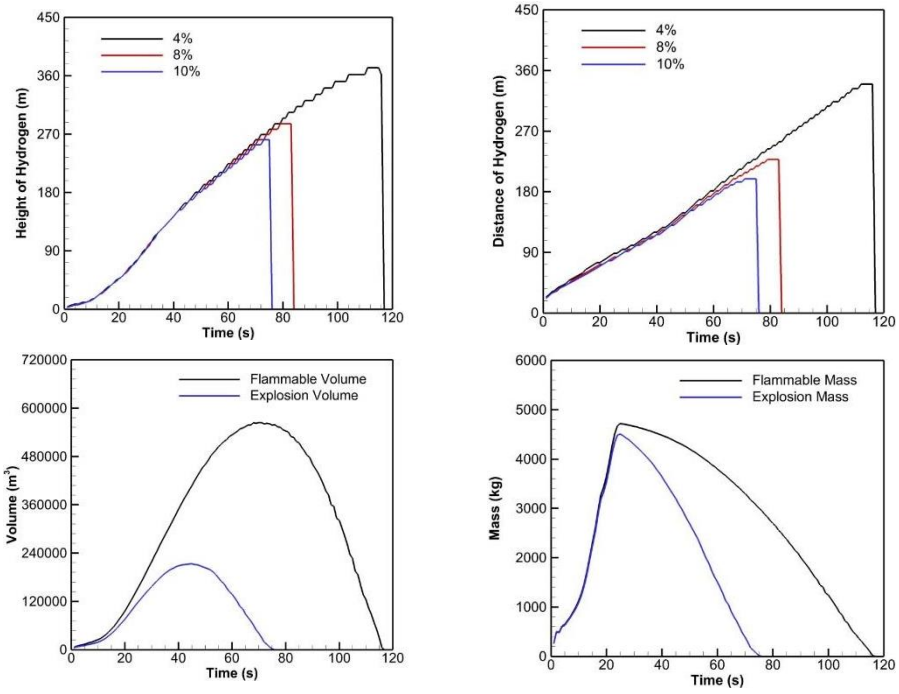

Fig. 5 The predicted 5 ton release under 3F conditions at ambient temperature 293K without retention pit.

In Fig. 5, a comparison is made between the predicted heights of the hydrogen cloud and horizontal extent in the case of a 5 ton release in 3F condition. The initial lift-off speed is approximately 3.4 m/s and dies out after 116 s. The initial travel speed is 2.8 m/s and the cloud travels as high as 380 m and as long as 340 m. The flammable cloud, i.e. the volume and mass of the hydrogen-air mixture within the flammability (4~75%) and explosive limits (18.3~59) are also plotted. The peak flammable hydrogen mass is roughly 94% of the total released mass. As a comparison, if the released hydrogen is 10 times the amount as shown in Fig. 6, The initial lift-off speed is approximately 3.9 m/s and dies out after 190 s. The initial travel speed is 2.6 m/s. The cloud travels as high as 600 m and as long as 500 m and the peak flammable hydrogen mass is still roughly 94% of the total released mass.

Subsequently, comparison is conducted for the cases with and without the retention pit. As shown in Fig.7, The cloud without a pit travels much higher and further than that with a pit. However, the cloud without a pit dies out more quickly than that with a pit. Figures 8 and 9 show that for 10 ton release under both 3F and 5D conditions at ambient temperature of 293 K, the predicted cloud sizes within the flammability and explosion limits are much larger for the cases without the retention pit.

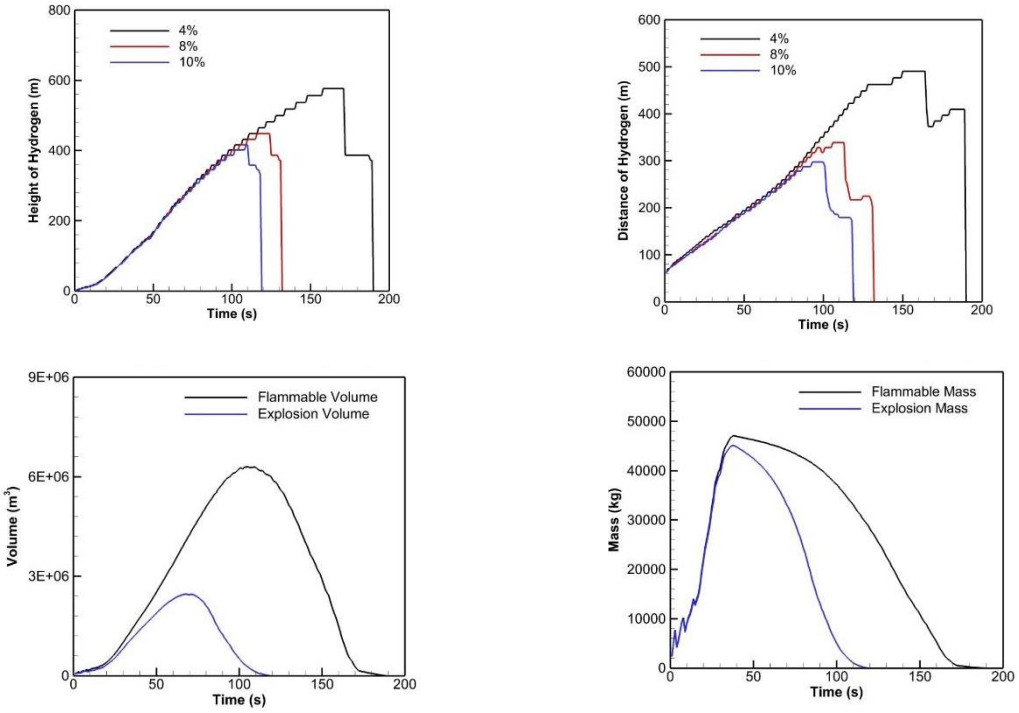

Fig. 6 The predicted 50 ton release under 3F conditions at ambient temperature 293K without retention pit.

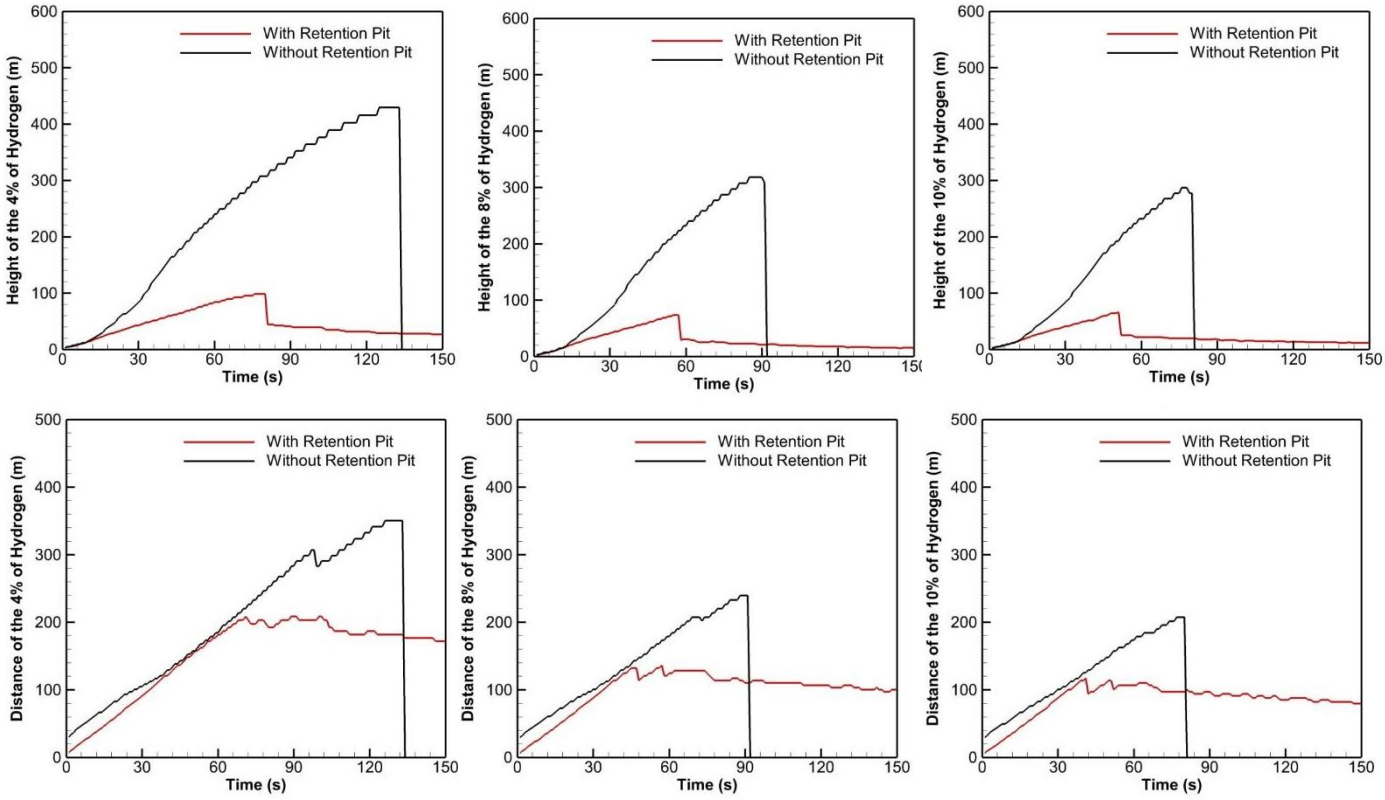

Fig. 7 Comparison of the cloud heights and horizontal extent with and without retention pit for 10 ton release scenario under 3F condition and 293 K.

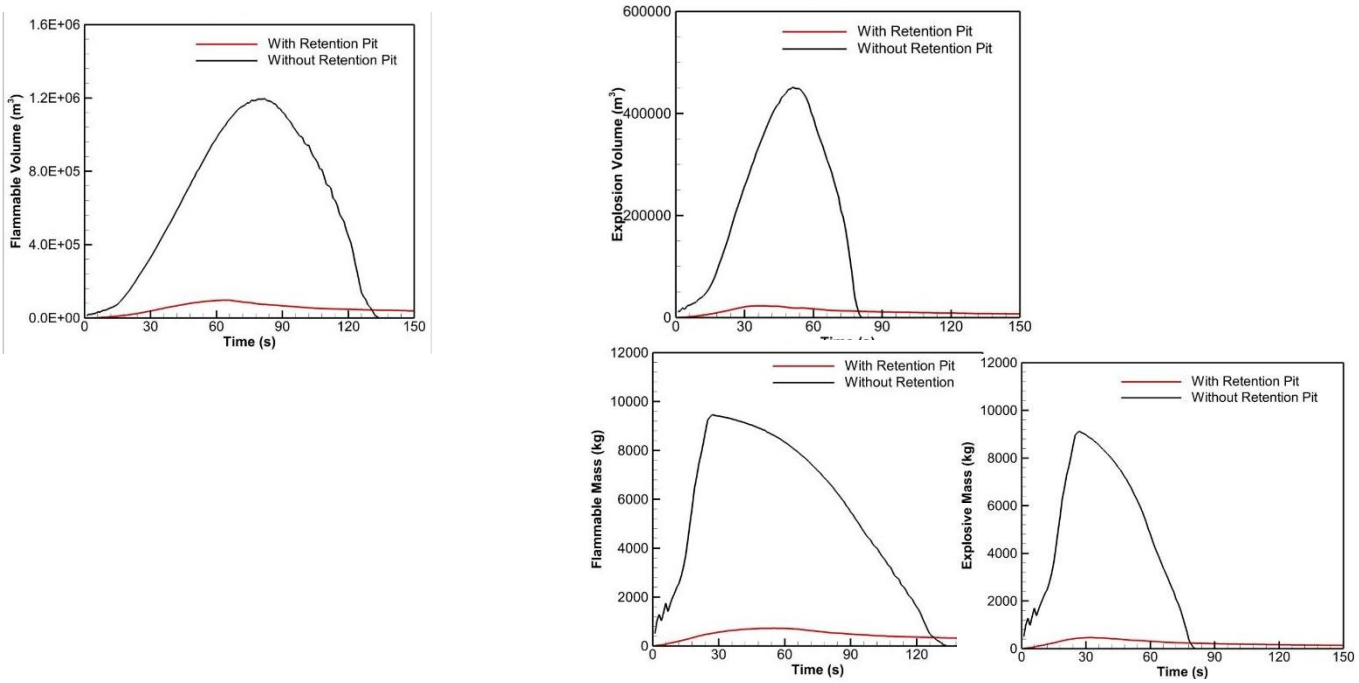

Fig. 8 Comparison of the predicted cloud sizes within the flammability and explosion limits for 10 ton release under 3F and ambient temperature of 293 K with and without retention pit.

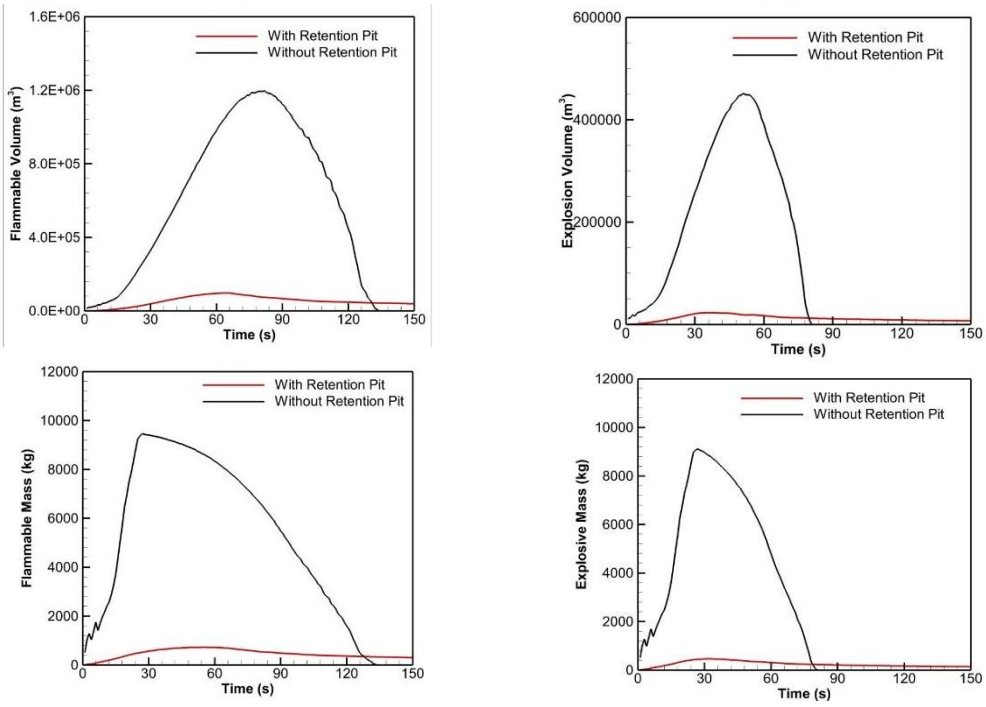

Fig. 9 Comparison of the predicted cloud sizes within the flammability and explosion limits for 10 ton release under 5D and ambient temperature of 293 K with and without retention pit.

Concluding remarks

The in-house dispersion code has been validated against NASA large-scale LH_2 dispersion, and the predictions agree well with the test data. Key influencing factors for the distribution of the dispersed cloud following liquid hydrogen release are found to include weather condition, wind speed and ambient temperature. More importantly, the retention pit has been found to have significant effect in reducing the vaporization rate, resulting in a smaller and long-lasting dispersed cloud. Without a retention pit, the dispersed cloud propagates higher from the ground and dies out quickly. According to the current study, although the retention pit can extend the dispersion time, it can significantly reduce the extent of hazards due to much smaller cloud size within both the flammability and explosion limits. While the former has negative impact on safety, the later is beneficial. The use of retention pit should hence be considered with caution in practical applications.

Acknowledgements

This work was funded by the UK Engineering and Physical Science Research Council (EPSRC) Impact Acceleration Accounts (IAAs) through the University of Warwick.

Reference

[1] Witcofski RD, Chirivella JE. Experimental and analytical analyses of the mechanisms governing the dispersion of flammable clouds formed by liquid hydrogen spills. Int J Hydrogen Energy 1984; 9(5): 425-35.

[2] https://www.engineeringtoolbox.com/convective-heat-transfer-d_430.html

[3] van den Bosch CJH, Weterings RAPM. Methods for the calculation of physical effects due to the release of hazardous materials (liquids and gases), CPR14E, TNO Yellow Book. 3rd ed. The Hague, The Netherlands:TNO; 1997.

[4] Pasquill, F. The estimation of the dispersion of windborne material, The Meteorological Magazine 1961, 90(1063): 33-49.